



## OPEN ACCESS

## EDITED BY

Hao Li,  
Jining Medical University, China

## REVIEWED BY

Alfonso Méndez-Bravo,  
National Autonomous University of Mexico,  
Mexico  
Da-Le Guo,  
Chengdu University of Traditional Chinese  
Medicine, China

## \*CORRESPONDENCE

Jian Xie  
✉ Xiejian@zmu.edu.cn  
Yuqi He  
✉ HYQJEFF@foxmail.com

RECEIVED 14 September 2023

ACCEPTED 13 November 2023

PUBLISHED 08 December 2023

## CITATION

Zhao Y, Ji X, Liu X, Qin L, Tan D, Wu D, Bai C,  
Yang J, Xie J and He Y (2023) Age-dependent  
dendrobine biosynthesis in *Dendrobium nobile*:  
insights into endophytic fungal interactions.  
*Front. Microbiol.* 14:1294402.  
doi: 10.3389/fmicb.2023.1294402

## COPYRIGHT

© 2023 Zhao, Ji, Liu, Qin, Tan, Wu, Bai, Yang,  
Xie and He. This is an open-access article  
distributed under the terms of the [Creative  
Commons Attribution License \(CC BY\)](#). The  
use, distribution or reproduction in other  
forums is permitted, provided the original  
author(s) and the copyright owner(s) are  
credited and that the original publication in this  
journal is cited, in accordance with accepted  
academic practice. No use, distribution or  
reproduction is permitted which does not  
comply with these terms.

# Age-dependent dendrobine biosynthesis in *Dendrobium nobile*: insights into endophytic fungal interactions

Yongxia Zhao<sup>1,2,3</sup>, Xiaolong Ji<sup>1,2,3</sup>, Xiaoqi Liu<sup>1,2,3</sup>, Lin Qin<sup>1,2,3</sup>,  
Daopeng Tan<sup>1,2,3</sup>, Di Wu<sup>1,2,3</sup>, Chaojun Bai<sup>4</sup>, Jiyong Yang<sup>5</sup>,  
Jian Xie<sup>1,2,3\*</sup> and Yuqi He<sup>1,2,3\*</sup>

<sup>1</sup>Guizhou Engineering Research Center of Industrial Key-Technology for *Dendrobium nobile*, Engineering Research Center of Pharmaceutical Orchid Plant Breeding, High Efficiency Application in Guizhou Province, Zunyi Medical University, Zunyi, China, <sup>2</sup>Key Laboratory of Basic Pharmacology of Ministry of Education, Joint International Research Laboratory of Ethnomedicine of Ministry of Education, Zunyi Medical University, Zunyi, China, <sup>3</sup>2011 Cooperative Innovation Center for Guizhou Traditional Chinese Medicine and Ethnic Medicine, Zunyi Medical University, Zunyi, China, <sup>4</sup>Guangxi Shenli Pharmaceutical Co., Ltd., Yulin, China, <sup>5</sup>Chishui Xintian Chinese Medicine Industry Development Co., Ltd., Zunyi, China

**Introduction:** *Dendrobium nobile* (*D. nobile*), a valued Chinese herb known for its diverse pharmacological effects, owes much of its potency to the bioactive compound dendrobine. However, dendrobine content varies significantly with plant age, and the mechanisms governing this variation remain unclear. This study delves into the potential role of endophytic fungi in shaping host-microbe interactions and influencing plant metabolism.

**Methods:** Using RNA-seq, we examined the transcriptomes of 1-year-old, 2-year-old, and 3-year-old *D. nobile* samples and through a comprehensive analysis of endophytic fungal communities and host gene expression in *D. nobile* stems of varying ages, we aim to identify associations between specific fungal taxa and host genes.

**Results:** The results revealing 192 differentially expressed host genes. These genes exhibited a gradual decrease in expression levels as the plants aged, mirroring dendrobine content changes. They were enriched in 32 biological pathways, including phagosome, fatty acid degradation, alpha-linolenic acid metabolism, and plant hormone signal transduction. Furthermore, a significant shift in the composition of the fungal community within *D. nobile* stems was observed along the age gradient. *Olpidium*, *Hannaella*, and *Plectosphaerella* dominated in 1-year-old plants, while *Strelitziana* and *Trichomerium* prevailed in 2-year-old plants. Conversely, 3-year-old plants exhibited additional enrichment of endophytic fungi, including the genus *Rhizopus*. Two gene expression modules (mediumpurple3 and darkorange) correlated significantly with dominant endophytic fungi abundance and dendrobine accumulation. Key genes involved in dendrobine synthesis were found associated with plant hormone synthesis.

**Discussion:** This study suggests that the interplay between different endophytic fungi and the hormone signaling system in *D. nobile* likely regulates dendrobine biosynthesis, with specific endophytes potentially triggering hormone signaling cascades that ultimately influence dendrobine synthesis.

## KEYWORDS

*Dendrobium nobile*, endophytic fungi, transcriptomic analysis, dendrobine, age-dependent accumulation

# 1 Introduction

*Dendrobium nobile* (*D. nobile*) is a precious medicinal herb found in the Danxia landform of Chishui City, Guizhou Province, China. It possesses a rich repertoire of bioactive compounds with notable antioxidant, anti-tumor, and immunomodulatory properties (Teixeira and Ng, 2017). *D. nobile* is considered a rare and valuable resource in Chinese herbal medicine, primarily obtained through wild-simulated cultivation. In its natural habitat, *D. nobile* thrives in clusters on Danxia rocks. Each cluster of *D. nobile* plants produces new stems and leaves every year, while the stems from previous years continue to grow. As a result, a cluster of *Dendrobium* plants may contain stems of 1-year-old, 2-year-old, 3-year-old and older ages. Interestingly, only the 1-year-old stems have leaves, while the older stems are leafless, and most of the 3-year-old stems produce new shoots at the nodes. Therefore, the age of the *Dendrobium* stems can be distinguished by these features. The chemical composition and content of Chinese herbs vary with different ages, and *D. nobile* is no exception (Lu et al., 2022).

However, the morphology and chemistry of plants are determined by a combination of gene expression and environmental factors. Environmental factors include not only light, humidity, temperature, etc., but also the microbial community within the plant, which is called endophyte and plays an important role in the plant's successional trajectory (Clay and Holah, 1999; Afkhami and Strauss, 2016), the balance between insects and plants, plant reproduction, and the accumulation of plant metabolites (Harrison et al., 2021). Interactions between symbiotic or parasitic microorganisms and their host plants are essential for maintaining plant homeostasis (Ma et al., 2021). Research in this area has entered a phase of rapid development, but our understanding of its microbe-hosts is still limited.

The main bioactive constituents of *D. nobile* are alkaloids, with dendrobine being a prominent compound regulated by the Pharmacopeia. Transcriptome analyzes have indicated that dendrobine is derived from the terpenoid-forming and indole pathways of the mevalonate pathway (MVA), the methylerythritol phosphate pathway (MEP), or the shikimate pathway (Wang et al., 2020). However, the details of these biosynthetic pathways to synthesize alkaloids are not well studied. We found that the content of dendrobine was closely related to the age of *D. nobile* and reached a maximum in the youngest 1-year-old plants. Moreover, we observed that the community and abundance of endophytes in 1-year-old *D. nobile* were significantly different from those in older plants. It has also been reported that some endophytic fungi can positively promote the accumulation of fatty acid metabolites in *D. nobile* by infestation and colonization (Zhao et al., 2023). Therefore, we hypothesize that endophyte colonization in 1-year-old *D. nobile* is closely related to the high content of dendrobine alkaloids. By performing transcriptome analysis on *D. nobile* samples of different ages, we identified a number of changes, including changes in some genes associated with the dendrobine synthesis pathway as well as changes in genes in other related pathways.

To validate this hypothesis, we conducted an extensive analysis of the endophytic fungal communities inhabiting *D. nobile* plants of varying ages and investigated their correlation with dendrobine content. Employing high-throughput sequencing technology, we identified and quantified the endophytic fungi residing within the stems of *D. nobile* plants. Subsequently, we performed a comprehensive analysis to determine the relationship between the relative abundance of specific fungal taxa and the levels of dendrobine present. Our

findings not only shed new light on the intricate involvement of endophytic fungi in the regulation of dendrobine synthesis and accumulation in *D. nobile* but also hold significant implications for the cultivation and utilization of this invaluable medicinal plant.

## 2 Materials and methods

### 2.1 Sample collection

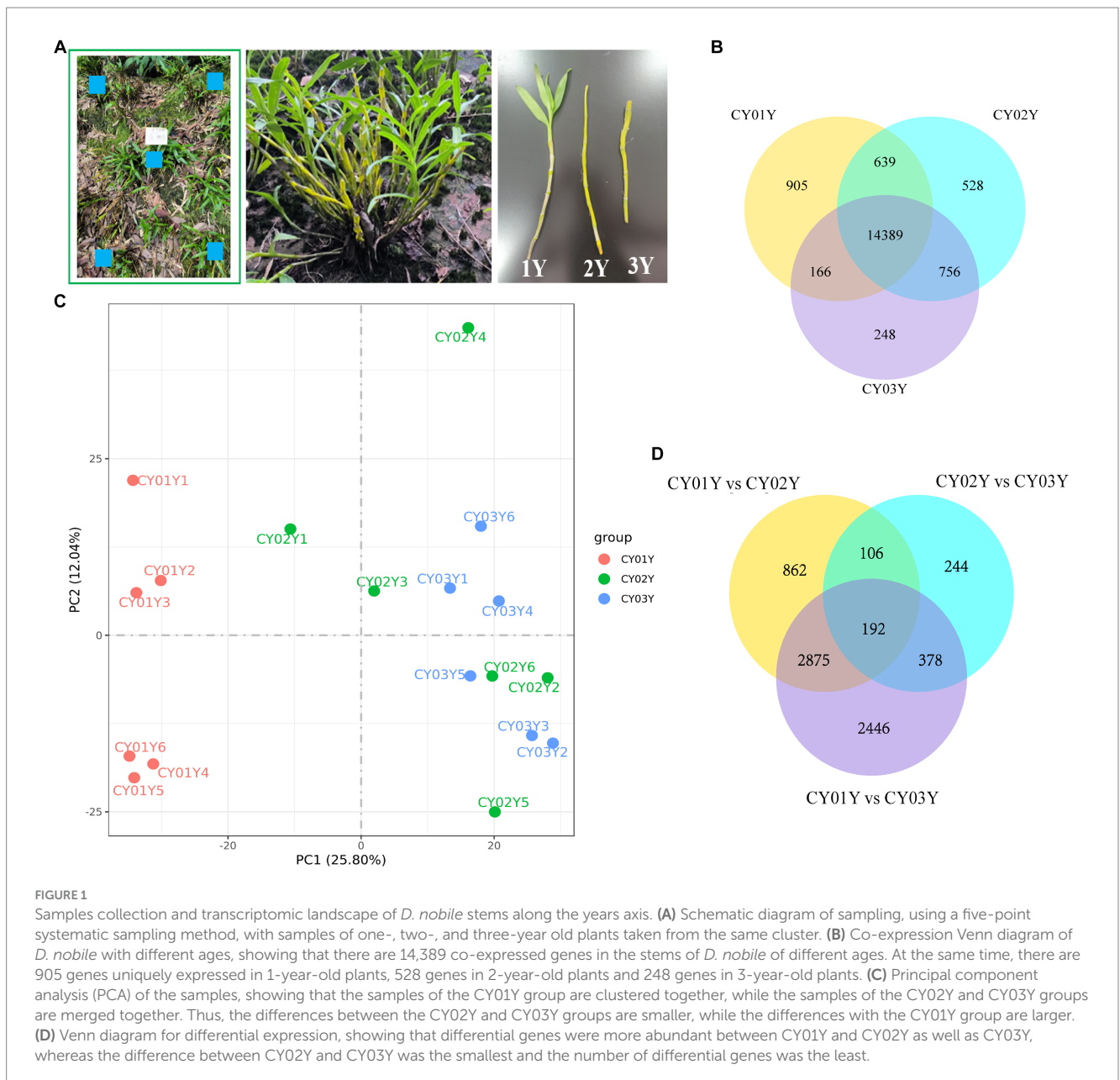
*D. nobile* stems of three age groups (1-year-old, 2-year-old and 3-year-old) in six biological replicates were collected from wild-simulated cultivation on Danxia rocks in ChiYan base in Chishui city, Guizhou (N 28°30'2", E 105°55'48") by using systematic sampling methods (Figure 1A). After the roots and leaves had been removed, the stems were divided into two parts: one part, containing 200 mg of each sample, was disinfected in the following way. First, the samples were immersed in 20 mL of 75% alcohol for 45 s. Second, after removing the alcohol, the samples were immersed in 20 mL of 0.1% mercuric chloride for 5 min. Finally, the samples were rinsed with sterile water three times to remove the remaining mercuric chloride. All of the stems were then sent to Novogene for the sequencing of the internal transcribed spacer (ITS) with  $-80^{\circ}\text{C}$  stored process. The other part of fresh *D. nobile* stems was flash-frozen in liquid nitrogen and transported on dry ice to Novogene for RNA extraction and subsequent experiments.

### 2.2 DNA extraction and sequencing of endophytic fungi

To characterize the endophytic fungal community in *D. nobile* stems of different ages, we employed the CTAB/SDS method for total genomic DNA extraction from each sample. The ITS genes were then amplified in specific regions using designated primers (Forward: GGAAGTAAAAGTTCGTAACAAGG; Reverse: GCTGCGTTCTCA TCGATGC) along with respective barcodes. Subsequently, we conducted library construction and sequencing on an Illumina NovaSeq platform, generating 250 bp paired-end reads following amplification, purification, and library construction as briefly outlined below: Amplification protocol:  $98^{\circ}\text{C}$  (1 min)  $\rightarrow$   $98^{\circ}\text{C}$  (10 s)  $\rightarrow$   $50^{\circ}\text{C}$  (30 s)  $\rightarrow$   $72^{\circ}\text{C}$  (30 s) (30 cycles)  $\rightarrow$   $72^{\circ}\text{C}$  (5 min). The PCR products were homogeneously combined and then subjected to purification using the Qiagen Gel Extraction Kit (Qiagen, Germany). For library preparation, we employed the NEBNext<sup>®</sup> Ultra<sup>™</sup> II DNA Library Prep Kit (Cat No. E7645). Subsequently, the library's quality was assessed utilizing the Qubit<sup>®</sup> 2.0 Fluorometer (Thermo Scientific) and the Agilent Bioanalyzer 2,100 system.

### 2.3 Transcriptome sequencing

To profile the transcriptomes of 18 stems from *D. nobile* of varying ages, we initiated the process by extracting total RNA from the plant samples. Subsequently, mRNA was isolated from the total RNA pool using poly-T oligo-attached magnetic beads. Prior to this, we employed the RNA Nano 6,000 Assay Kit on the Bioanalyzer 2,100 system to evaluate RNA integrity. Of paramount importance was the



initiation of first strand cDNA synthesis, where a combination of random hexamer primers and M-MuLV Reverse Transcriptase (RNase H-) played a crucial role. Following this, DNA Polymerase I and RNase H were enlisted to synthesize the second strand of cDNA. The pivotal step in this process was library construction. Here, the AMPure XP system (Beckman Coulter, Beverly, United States) was utilized to meticulously purify and select cDNA fragments falling within the 370~420 bp range. Finally, the library preparations were subjected to sequencing on an Illumina Novaseq platform.

## 2.4 Data analysis of ASVs of endophytic fungi

The 18 samples were sequenced on the Illumina NovaSeq platform. We processed the raw reads by removing the barcodes and primer sequences according to barcode sequences. Paired-end reads

were merged using FLASH.<sup>1</sup> To obtain high-quality Clean Tags, we used the fastp (Version 0.20.0) software to filter out low-quality reads. The Vsearch (Version 2.15.0) was used to detect the chimeric sequences, and then the chimeric sequences were removed to obtain the Effective Tags. ASVs Denoise and species annotation was realized in the QIIME2 software (Version QIIME2-202006), and then ASVs with abundance less than 5 were filtered out. The ASVs absolute abundance was normalized using a standard of sequence number corresponding to the sample with the least sequences. Subsequent analysis of alpha diversity and beta diversity were all performed based on the normalized data and calculated in QIIME2. Principal Coordinate Analysis (PCoA) was performed with QIIME2 package, ade4 package and ggplot2 package in R software (Version 3.5.3). To

<sup>1</sup> Version 1.2.11, <http://ccb.jhu.edu/software/FLASH/>

identify the significantly different taxa at each taxonomic level (Phylum, Class, Order, Family, Genus, Species), T-test analysis was performed using R software (Version 3.5.3).

## 2.5 Data analysis of RNA-Seq

Clean data (clean reads) in fastq format was first processed by fastp software to remove adapter, poly-N and low-quality reads. The high-quality clean data was then analyzed for Q20, Q30 and GC content. Hisat2 v2.0.5 and StringTie (v1.3.3b) were adopted to map reads to the reference genome and predict novel transcripts. The number of reads mapped to each gene was counted using Feature Counts v1.5.0-p3. Finally, the FPKM (fragments per kilobase of transcript per million mapped reads) of each gene was calculated. FPKM provides a normalized measure of gene expression, factoring in sequencing depth and gene length, and is widely adopted for estimating gene expression levels. Differential expression analysis was performed between two groups, each consisting of two biological replicates per condition, using the DESeq2 R package (1.20.0). DESeq2 employs statistical routines based on the negative binomial distribution to determine differential expression in digital gene expression data. The resulting  $p$ -values were adjusted using the Benjamini and Hochberg's approach to control the false discovery rate. Genes with an adjusted  $p$ -value of  $\leq 0.05$ , as determined by DESeq2, were identified as differentially expressed. Gene Ontology (GO) enrichment analysis of differentially expressed genes was implemented by the clusterProfiler R package, then to test the statistical enrichment of differentially expressed genes in KEGG pathways.<sup>2</sup> Eventually, WGCNA (Weighted correlation network analysis) was performed through the R package WGCNA.

## 3 Results

### 3.1 Different transcriptomic landscapes in developmental gradients along the year axis

In this study, we examined the *Dendrobium nobile* stems (Figure 1A) from three distinct age groups: 1-year-old seedlings with leaves (CY01Y), 2-year-old bare stems without leaves (CY02Y), and 3-year-old stems that have sprouted (CY03Y). We conducted both a transcriptomics experiment and an endogenous fungi analysis. Gene expression in the stems of all 18 samples (with six biological replicates per age group) was assessed, and it is noteworthy that all samples exhibited comparable read counts (averaging 42,895,882, 41,514,350, and 44,681,382 clean reads, respectively). Additionally, all samples maintained an average quality score exceeding 30 phred (Supplementary Table S1).

The co-expression Venn diagram (Figure 1B) demonstrated that 905 genes were uniquely expressed in 1-year-old plants, 528 genes in 2-year-old plants, and 248 genes in 3-year-old plants. Moreover, a substantial overlap of 14,389 genes was observed across all three age groups. Principal component analysis (PCA) and differential gene

analysis (Figures 1C,D) further illustrated the high degree of transcriptomic similarity between 2- and 3-year-old plants when compared to the 1-year-old plants.

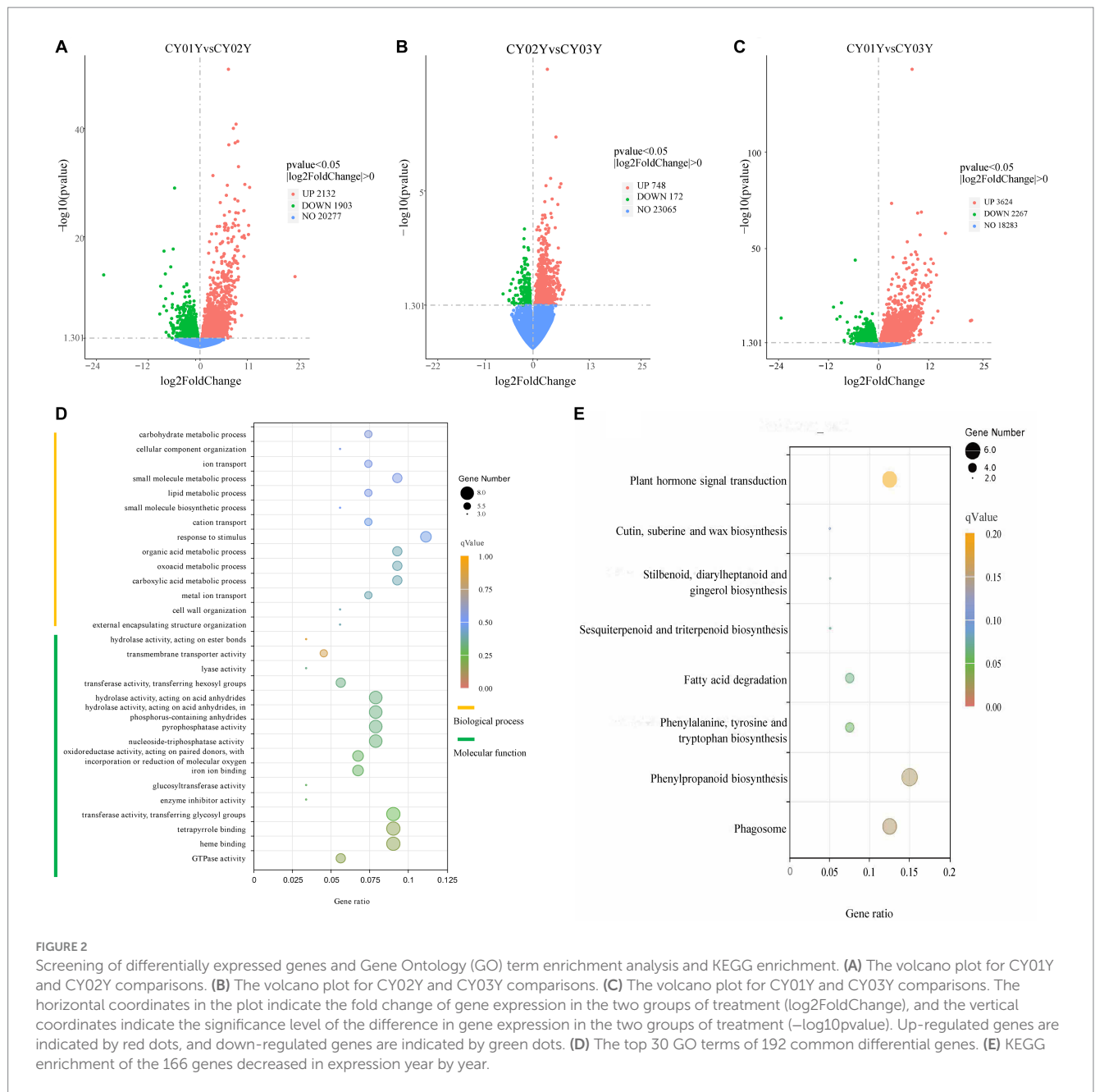
To examine gene expression disparities, read counts from the 18 samples underwent DESeq2 analysis. Our analysis identified 4,035 differentially expressed genes between 1-year-old and 2-year-old plants, 5,891 differentially expressed genes between 1-year-old and 3-year-old plants, and 920 differentially expressed genes between 2-year-old and 3-year-old plants at  $p < 0.05$  (Figure 2). Among them gene, 2,132 (52.8%) were up-regulated and 1,903 (47.2%) were down-regulated in annual and biennial *D. nobile* (Figure 2A). Similarly, the expression of 3,624 (61.5%) genes was up-regulated and 2,267 (38.5%) genes were down-regulated in one-year plants as compared to three-year plants (Figure 2B). However, fewer differential genes were identified between 2-year and 3-year plants, with only 748 (81.3%) genes up-regulated and 172 (18.7%) genes down-regulated in expression (Figure 2C). A Venn diagram of the commonly expressed differential genes between the different years of *D. nobile* stems revealed 192 common differential genes in the three sets of samples (Figure 1D).

For a deeper understanding of the functional distinctions among differentially expressed genes, we conducted Gene Ontology (GO) term enrichment analysis. Twenty-five genes were annotated to 154 biological processes, encompassing external encapsulating structure organization, cell wall organization, glucan metabolic processes, carboxylic acid metabolic processes, and others. Three genes were annotated to 16 cellular components including cell wall, external encapsulating structure, apoplast extracellular region, etc. Notably, differential genes were predominantly localized in the cell wall and organelles within the cytoplasm. Furthermore, 44 genes were annotated to 93 molecular functions, such as GTPase activity, heme binding, tetrapyrrole binding, transferase activity, enzyme inhibitor activity, glucosyltransferase activity, and others (Supplementary Table S2). Among the top 30 annotated GO terms, molecular function accounted for 53 percent while biological processes accounted for 47 percent (Figure 2D). Analyzing the 192 screened genes (Supplementary Table S3) through heatmap clustering, we observed that 166 genes exhibited a gradual decrease in expression year by year, while only 10 genes displayed a gradual increase in expression with age. The highest expression was observed in the 2-year-old plants, consistent with another 16 genes (Supplementary Figure S1). Subsequently, KEGG enrichment analysis of the three groups of differential genes revealed that group A differential genes were predominantly enriched in 32 biological pathways, including Phagosome, Phenylpropanoid biosynthesis, Phenylalanine metabolism, Fatty acid degradation, alpha-Linolenic acid metabolism, Plant hormone signal transduction, Sesquiterpenoid and triterpenoid biosynthesis, Biosynthesis of unsaturated fatty acids, and others (Figure 2E).

### 3.2 Endophytic fungal community composition in the stems shifts along the age axis

In this study, we thoroughly examined the distribution of endophytic fungal taxa in *D. nobile* stems across different age groups through internal transcribed spacer sequencing, complemented by a

<sup>2</sup> <http://www.genome.jp/kegg/>

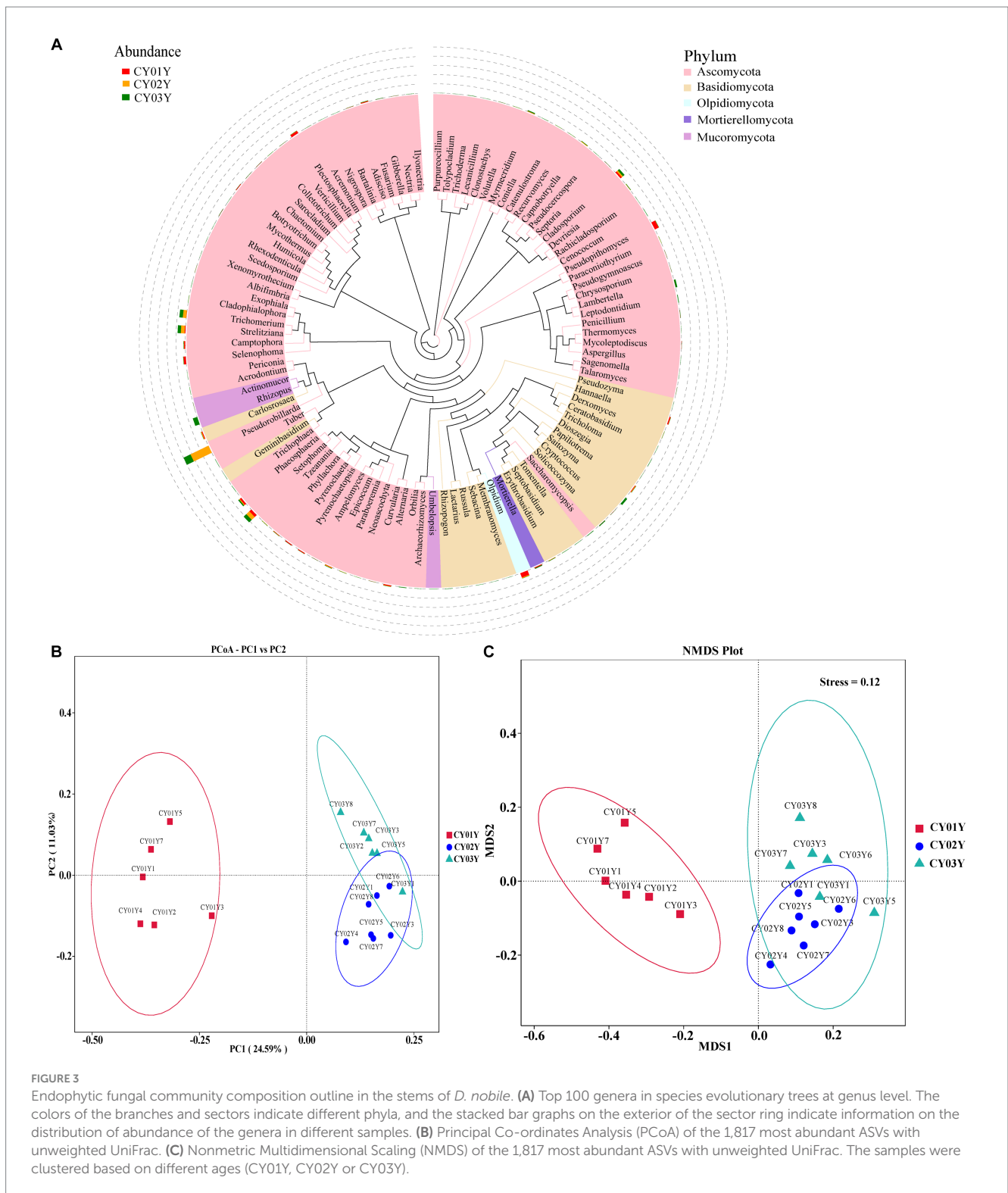


detailed analysis of the fungal microbiomes (Methods). The systematic sampling approach (Figure 1A) was validated by rarefaction analysis, affirming the sequencing depth was sufficient to capture the majority of endophytic fungal members in all 18 stem samples (Supplementary Figure S2). A total of 1.72 million Effective Tags underwent analysis using QIIME2, leading to the identification of 1,817 Amplicon Sequence Variants (ASVs) at a 100% identity level. The overall analysis demonstrated discernible distinctions among the three age groups (Figures 3A, 4A2).

Principal Co-ordinates Analysis (PCoA) (Figure 3B) and Nonmetric Multidimensional Scaling (NMDS) (Figure 3C) of the 1,817 most abundant ASVs based on unweighted UniFrac and nonphylogenetic Bray-Curtis metrics (Adonis  $p$  value = 0.001) unveiled a notable shift in fungal community composition within *D. nobile* stems across the age gradient. Both PCoA and NMDS plots

highlighted distinct clustering based on age groups (CY01Y, CY02Y, or CY03Y). Alpha diversity metrics, including Chao1, observed OTUs, Shannon, and Simpson indices, indicated a balanced overall biodiversity of endophytic fungi across all samples (Figure 5).

We further investigated taxonomic differences in abundance among the endophytic microbiomes of CY01Y, CY02Y, and CY03Y plants using phyloseq. Eight phyla and 20 classes, orders, and genera were selected for analysis at different taxonomic ranks. Among them, 20 highly abundant ASVs exhibited significant differences between CY01Y, CY02Y, and CY03Y (Figure 4). Ternary plots and abundance accumulation diagrams of endophytic fungi in *D. nobile* stems across different ages were generated to visualize dominant taxa variations (Figure 4). Ascomycota exhibited the highest abundance in all samples, with significant enrichment in 2-year-old and 3-year-old *D. nobile* stems. Basidiomycota displayed a similar trend.



Mucoromycota were particularly abundant in 3-year-old samples, whereas Mortierellomycota were nearly absent in 2-year-old samples (Figures 4A1,A2).

At the genus level, *Pseudorobillarda* showed significant enrichment in 2-year-old and 3-year-old *D. nobile* stems, with markedly higher abundance in the 2-year-old plants compared to the 3-year-old ones. Conversely, *Pseudopithomyces* was enriched

exclusively in 1-year-old samples and absent in 2- and 3-year-old samples. Several fungi were specifically enriched in 1-year-old samples, including *Pyrenochaeta*, *Plectosphaerella*, *Selenophoma*, *Olpidium*, and *Hannaella*, while no fungi were specifically enriched in 2-year-old stems. Three genera, *Rhizopus*, *Lambertella*, and *Saccharomycopsis*, exhibited higher abundance in 3-year-old samples compared to the other groups (Figures 4E1,E2). The T-test

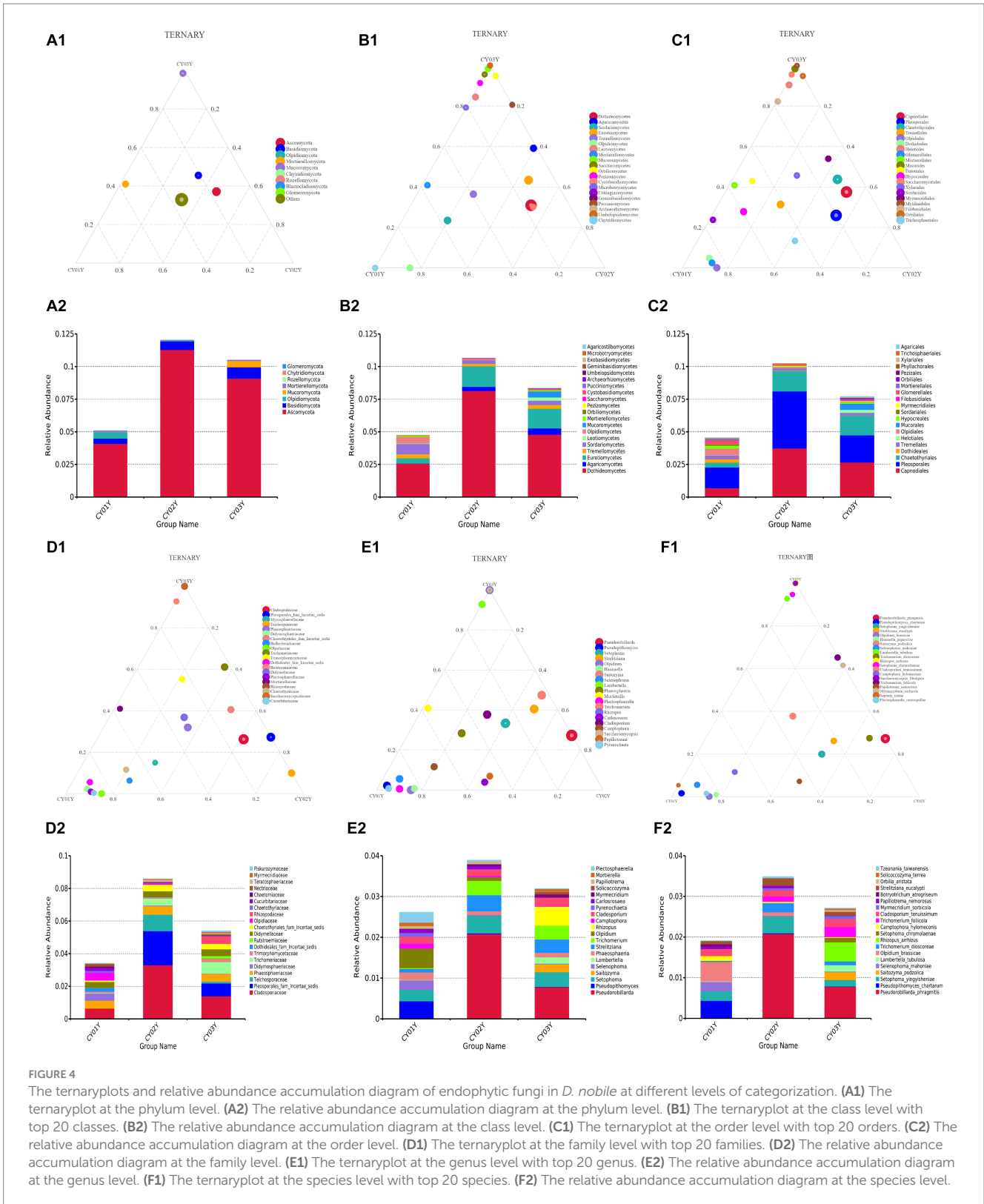
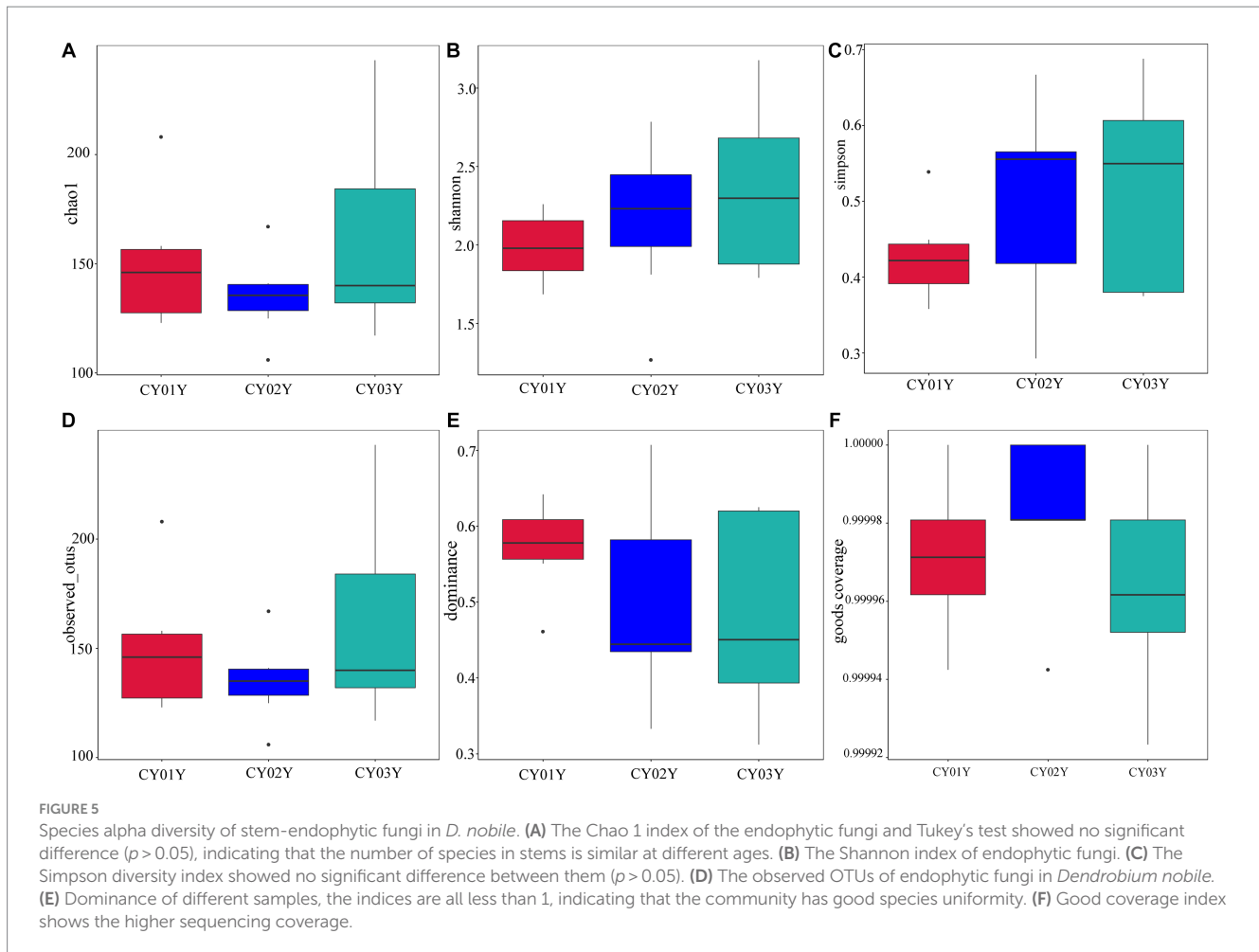


FIGURE 4

The ternaryplots and relative abundance accumulation diagram of endophytic fungi in *D. nobilis* at different levels of categorization. (A1) The ternaryplot at the phylum level. (A2) The relative abundance accumulation diagram at the phylum level. (B1) The ternaryplot at the class level with top 20 classes. (B2) The relative abundance accumulation diagram at the class level. (C1) The ternaryplot at the order level with top 20 orders. (C2) The relative abundance accumulation diagram at the order level. (D1) The ternaryplot at the family level with top 20 families. (D2) The relative abundance accumulation diagram at the family level. (E1) The ternaryplot at the genus level with top 20 genus. (E2) The relative abundance accumulation diagram at the genus level. (F1) The ternaryplot at the species level with top 20 species. (F2) The relative abundance accumulation diagram at the species level.

results demonstrated higher similarity in endophytic fungi between 2-year-old and 3-year-old plants, while 1-year-old plants exhibited greater dissimilarity, aligning with the differences observed between 2-year-old and 3-year-old plants. Fungal genera significantly enriched in annuals were *Olipidium*, *Hannaella*, and

*Plectospherella*, whereas endophytic fungi *Strelitziana* and *Trichomerium* were most enriched in biennials. Perennials were enriched in endophytes, including *Rhizopus*, with only a single addition compared to the biennials, while the rest remained consistent (Figure 6).

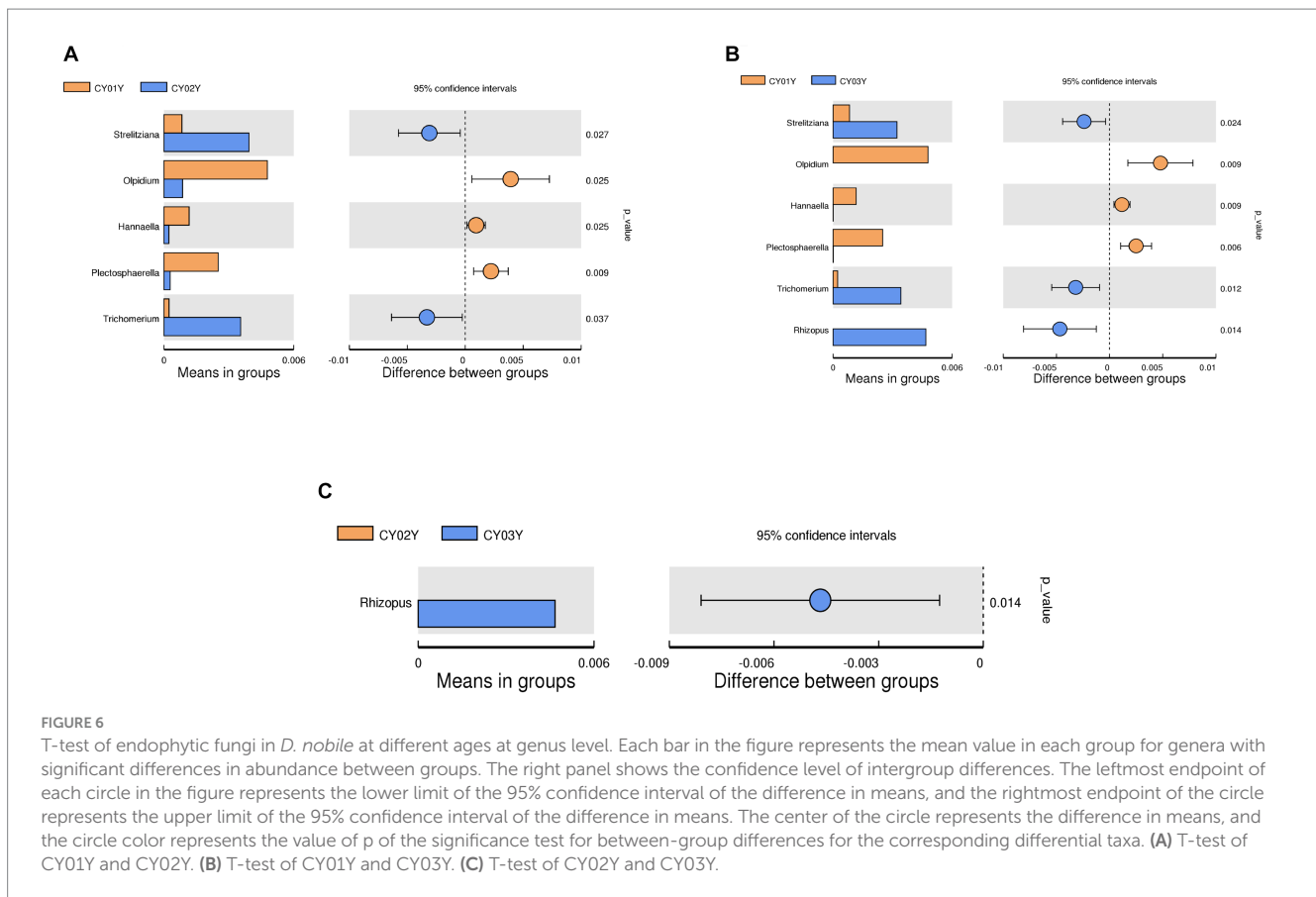


To probe into the relationships between stem genotype and age-dependent fungal ASVs in endophytic fungi, we constructed a co-abundance network. In line with PCA data, endophytic fungal ASVs exhibited intricate networks, providing insights into interactions between fungal communities at different age states. Notably, distinctive differences were observed in the community structures of microbes associated with 1-year-old stems versus those associated with 2- or 3-year-old stems. For microbes linked with 1-year-old stems, Spearman correlation analysis identified 17 species with a correlation above a threshold of 0.2 ( $p < 0.01$ ; Figure 7A). Positive correlations were observed, such as *Pseudophthomyces* with *Pyrenochaeta*, *Phaeosphaeria*, and *Setophoma*, as well as *Septoria* with *Trichomerium* and *Fusarium*. Additionally, there were pairwise correlations between *Albifimbria* and *Myrmecridium*, *Lambertella* and *Mycocleptodiscus*, and *Botryotrichum* and *Solicoccozyma*. However, *Phyllachora* exhibited a negative correlation with *Papiliotrema*. For microbes associated with 2-year-old stems, Spearman correlation analysis revealed 16 taxa with a correlation above a threshold of 0.2 ( $p < 0.01$ ; Figure 7B). Positive correlations were observed among *Pyrenochaetopsis*, *Carlosrosaea*, and *Hannaella*; *Phyllachora*, *Phaeosphaeria*, and *Setophoma*; and *Olpidium*, *Plectosphaerella*, and *Papiliotrema*. Additionally, there was a positive correlation between *Alternaria* and *Catenulostroma*, as well as *Epicoccum* with *Pseudorobillarda*, *Camptophora*, and *Cladosporium*. Furthermore, *Camptophora* showed a positive correlation with *Trichomerium*, while

*Alternaria* showed a positive correlation with *Catenulostroma*. Thirteen species exhibited significant Spearman correlation with 3-year-old stems (Spearman  $> 0.2$ ,  $p < 0.05$ ; Figure 7C). Among them, nine taxa (*Tomentella*, *Trichoderma*, *Mortierella*, *Tomentella*, *Saitozyma*, *Solicoccozyma*, *Cenococcum*, *Penicillium*) positively correlated with each other. The other two taxa groups *Pseudophthomyces* and *Epicoccum*, *Fusarium* and *Capnobotryella* also positively correlated.

### 3.3 Association of the stem transcriptome and endophytic fungi across different ages

The stem RNA-sequencing (RNA-seq) reads and microbial amplicon reads underwent stringent filtering to establish significant correlations of the factors ages, genes, and fungi between the datasets, thereby associating gene expression with fungi ASV abundance. Utilizing WGCNA analysis on all genes in the unigenes of the RNA-Seq data, 24 modules were delineated (weighting factor  $\beta = 10$  and Height of Clustering of module eigengenes was 0.3). Among these, 16,441 genes were enriched in 23 modules, while 34 genes were not enriched in these modules and were cataloged as gray modules, resulting in a total of 24 modules (Supplementary Table S5; Figure 8A). The distribution of genes within each module is illustrated in Figure 8B.



Pearson correlation coefficients and environmental factors were computed for the Module Eigengenes (MEs) of all modules to identify modules associated with environmental factors (Figure 8C). The mediumpurple3 module exhibited a significant correlation with the endophytic fungal genera *Olpidium* ( $R=0.58$ ,  $p=0.01$ ), *Hannaella* ( $R=0.72$ ,  $p=8e-04$ ), and *Plectosphaerella* ( $R=0.43$ ,  $p=0.07$ ). Similarly, the darkorange module demonstrated a significant correlation with the endophytic fungal genera *Olpidium* ( $R=0.73$ ,  $p=5e-04$ ), *Hannaella* ( $R=0.65$ ,  $p=0.004$ ), and *Plectosphaerella* ( $R=0.86$ ,  $p=5e-06$ ). Additionally, the greenyellow module exhibited a significant correlation with the endophytic fungal genera *Strelitziana* ( $R=0.63$ ,  $p=0.005$ ) and *Trichomerium* ( $R=0.64$ ,  $p=0.005$ ), while showing a significantly lower correlation with the endophytic fungal genus *Rhizopus* (Figure 8C).

Subsequently, module membership (MM) was assessed to determine the correlation between genes and specific modules. Correlation analyzes were conducted between the Gene Significance (GS) of significantly different endophytic fungi and the MM of each modular gene to ascertain if the MM values closely aligned with these endophytes, as well as dendrobine content. The outcomes revealed that in the darkorange module, the correlation coefficient between GS for *Olpidium*, *Hannaella*, and *Plectosphaerella* and MM was the highest. The correlation coefficients were  $\text{cor}=0.71$ ,  $p=2e-160$ ;  $\text{cor}=0.57$ ,  $p=9.9e-91$ ;  $\text{cor}=0.83$ ,  $p<1e-200$ . Furthermore, in the greenyellow module, the correlation coefficients between the GS for endophytic fungi *Strelitziana* and *Trichomerium* and MM were the highest ( $\text{cor}=0.52$ ,  $p=3.7e-25$ ;  $\text{cor}=0.47$ ,  $p=3e-20$ ; Figure 9B).

To elucidate hub genes associated with the predominant endophytic fungi in 1-year-old *D. nobile* stems, the mediumpurple3 and darkorange modules were filtered based on Gene Significance (GS) and Module Membership (MM) values with a threshold of 3. The selected genes were then imported into Cytoscape, and the top 10 hub genes were identified using the cytoHubba plugin (Figures 8D,E). Among these genes, KFK09\_024202 is a cell wall structural protein gene, KFK09\_000278 is a CRIB domain-containing protein gene, KFK09\_002541 is an mRNA of laccase-3, KFK09\_000072 is an mRNA of probable polygalacturonase, KFK09\_012583 is a HIP41 ARATH Heavy metal-associated isoprenylated plant protein gene, KFK09\_002946 is a TOR1 ARATH Microtubule-associated protein gene, KFK09\_021863 is a PMI11\_ARATH Pectinesterase inhibitor coding mRNA, and KFK09\_021567 is a KATAM\_ORYSJ Xyloglucan galactosyltransferase gene (Figure 10).

For an in-depth analysis of the association of the greenyellow module with dominant endophytic fungi in 2- and 3-year-old *D. nobile*, 10 hub genes in the greenyellow module were selected based on GS and MM values, with a focus on  $\text{MM}>0.8$  and  $\text{GS}>0.2$ . These hub genes exhibited significantly higher expression in 2- and 3-year-old plants compared to 1-year-old plants. Additionally, they exhibited a consistent trend of expression with the endophytic fungi *Trichomerium* and *Strelitziana* in *D. nobile* stems (Figure 11).

Consequently, it can be inferred that the gene expression modules significantly associated with the dominant endophytes of *D. nobile* are the mediumpurple3 and darkorange modules, correlating with different plant ages. The predominant fungi in young 1-year-old stems belong to the genera *Olpidium*, *Hannaella*, and *Plectosphaerella*,

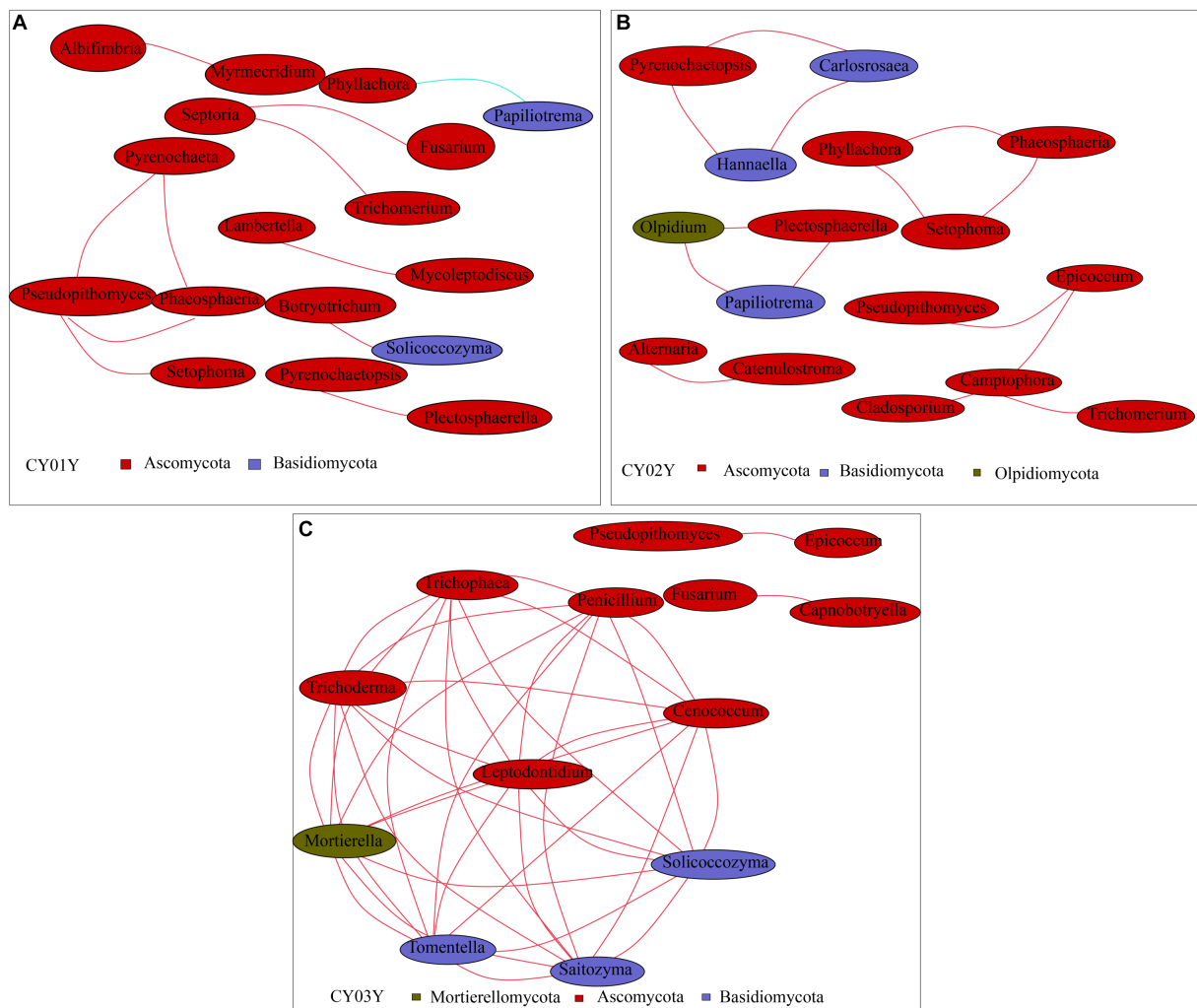


**FIGURE 7** Co-occurrence network of age-associated ASVs selected. Different nodes represent different genera, node size represents the average relative abundance of the genus, nodes of the same phylum are of the same color (as shown in the legend), the thickness of the lines between the nodes is positively correlated with the absolute value of the correlation coefficient of the species interactions, and the color of the lines corresponds to the positive and negative correlation (red positive correlation, blue negative correlation). (A) Co-occurrence network of CY01Y. (B) Co-occurrence network of CY02Y. (C) Co-occurrence network of CY03Y. The key parameters in Network Diagram such as Network Diameter (ND), Modularity Degree (MD), Clustering Coefficient (CC), Graph Density (GD), Average Degree (AD), Average Path Length (APL) are shown in [Supplementary Table 4](#).

exhibiting positive correlations with the mediumpurple3 and darkorange modules. Conversely, the dominant endophytic fungi expressed in older 2- and 3-year-old stems pertain to *Trichomerium* and *Strelitziana* species, and are significantly and positively correlated with the greenyellow module.

### 3.4 Age-dependent changes in the stem transcriptome and endophytic fungi are synchronized with properties of synthetic dendrobine in plants

Furthermore, we investigated whether the decline in dendrobine content with age is associated with age-specific transcriptome characterization in interaction with endophytic fungi. The 1-year-old stems of *D. nobile* exhibited the highest accumulation of dendrobine (Figure 9A). Through WGCNA analysis of the transcriptomes of

*Dendrobium* stems of three different ages, we identified four modules - mediumpurple3 ( $R=0.78, p=2e-04$ ), darkorange ( $R=0.75, p=3e-04$ ), honeydew1 ( $R=0.61, p=0.008$ ), and yellow ( $R=0.64, p=0.004$ ) - that demonstrated a significant positive correlation with dendrobine content. In contrast, the greenyellow module ( $R=-0.97, p=7e-11$ ) displayed a significant negative correlation with dendrobine content. Subsequently, we conducted a correlation analysis between the GS of dendrobine content and MM of genes in each module to examine their relationship with dendrobine content. The highest correlation coefficients between GS of dendrobine content and MM were observed in the greenyellow, followed by the mediumpurple3 and darkorange modules, with correlation coefficients of  $cor=0.94, p=2.6e-161$ ;  $cor=0.77, p=1e-200$ ; and  $cor=0.66, p=3.3e-131$  (Figure 9B). Given its significant negative correlation with dendrobine, the greenyellow module was not further analyzed.

The mediumpurple3 and darkorange modules were then subjected to GO functional enrichment. The mediumpurple3 module was

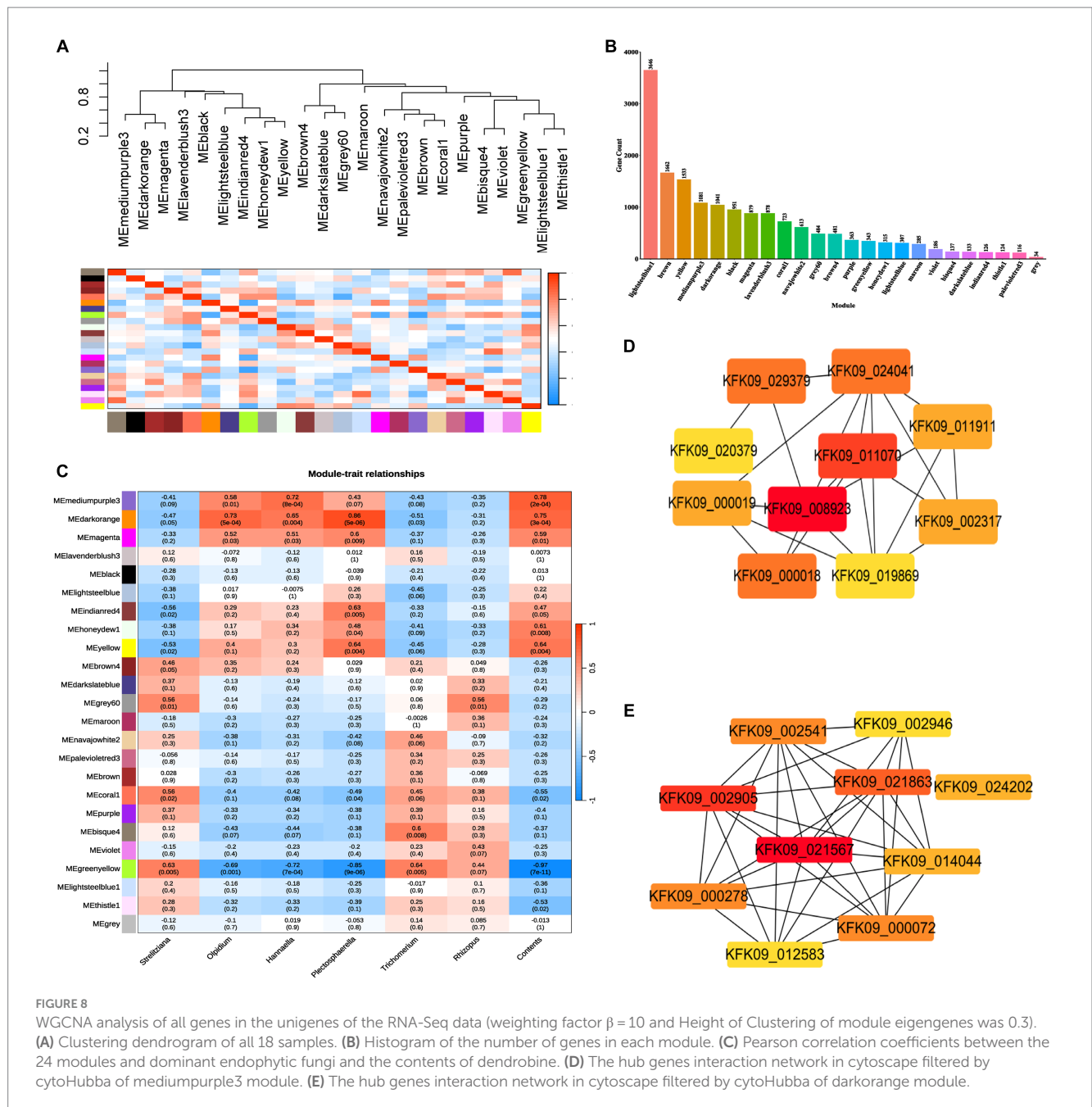


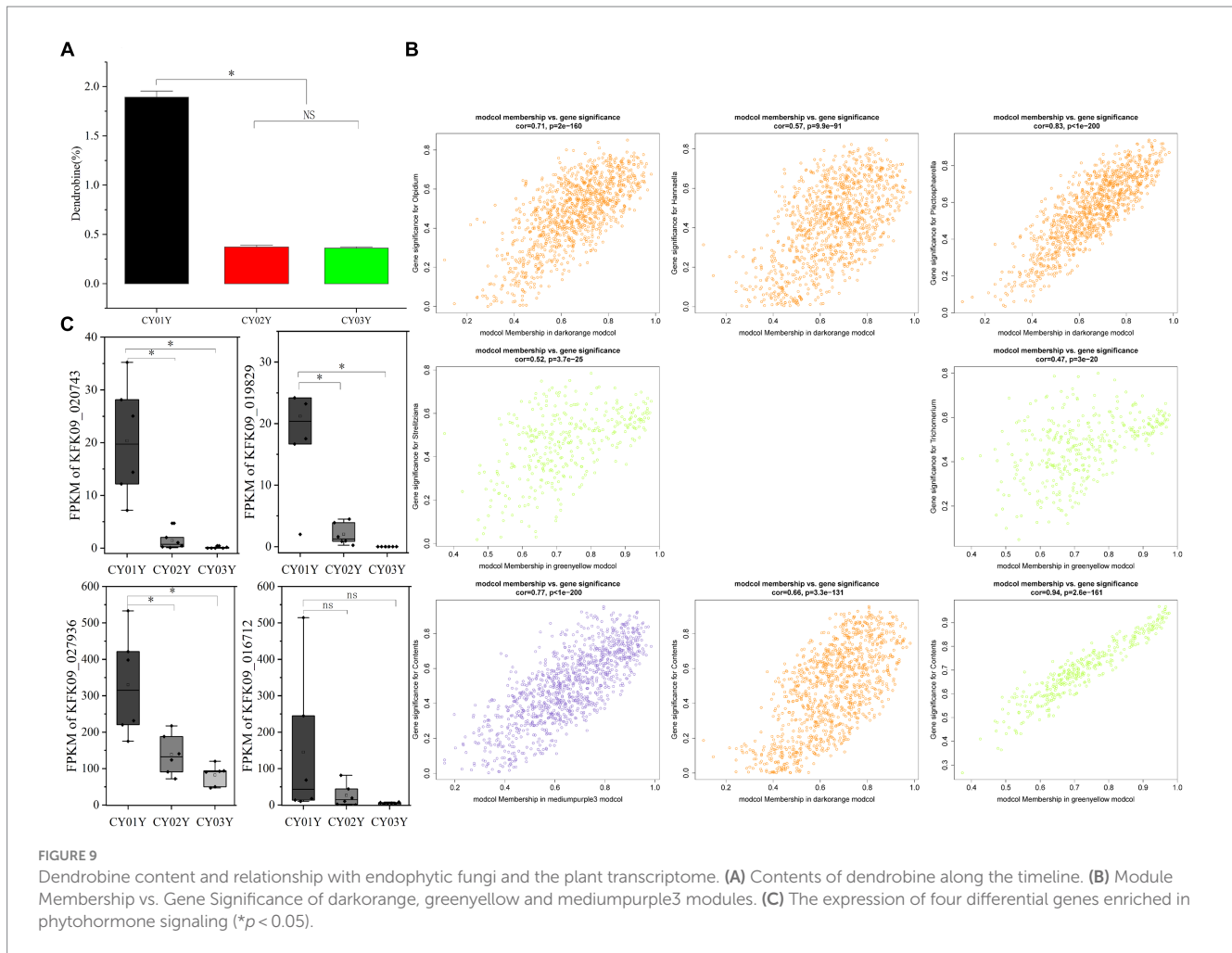
**FIGURE 8** WGCNA analysis of all genes in the unigenes of the RNA-Seq data (weighting factor  $\beta = 10$  and Height of Clustering of module eigengenes was 0.3). **(A)** Clustering dendrogram of all 18 samples. **(B)** Histogram of the number of genes in each module. **(C)** Pearson correlation coefficients between the 24 modules and dominant endophytic fungi and the contents of dendrobine. **(D)** The hub genes interaction network in cytoscape filtered by cytoHubba of mediumpurple3 module. **(E)** The hub genes interaction network in cytoscape filtered by cytoHubba of darkorange module.

primarily enriched for processes related to carbohydrate metabolism and transferase activity, while the darkorange module exhibited enrichment in processes associated with transferase activity and oxidoreductase activity (Supplementary Figure S3). However, only a few genes in the modules related to endophytic fungi showed significant enrichment in GO functions. This indicates that dissimilarity in gene expression does not always correspond to functional diversity.

Specifically, among the hub genes identified in these modules, only KFK09\_002541, KFK09\_000072, and KFK09\_021863 were enriched in GO functional categories related to oxidation–reduction processes, carbohydrate metabolism, and enzyme inhibitor activity. Notably, no significant direct correlation with the dendrobine synthesis pathway was observed. Since alkaloid synthesis has been

reported to correlate with the phytohormone pathway (Yan et al., 2019), we also examined four differential genes enriched in phytohormone signaling at different age gradients (gene-KFK09\_020743, gene-KFK09\_019829, gene-KFK09\_027936, gene-KFK09\_016712) categorized in the mediumpurple3 module. While these genes were not selected as core genes by WGCNA, they were listed as hub genes due to their functional significance (Figure 9C).

In addition, it's crucial to consider the reported changes in the expression of genes involved in the dendrobine synthesis pathway. The MVA pathway and the MEP pathway are the most documented biogenic pathways for dendrobine synthesis (Gong et al., 2021). Our data mining identified relevant genes in the MVA pathway, including acetoacetyl-CoA thiolase (AACT), 3-hydroxy-3-methylglutaryl-CoA synthase (HMGS), mevalonate kinase (MK), phosphomevalonate



kinase (PMK), mevalonate diphosphate decarboxylase (MVD), farnesyl diphosphate synthase (FPPS), and others. Genes that displayed a similar trend to dendrobine content included the HMGR genes KFK09\_028710, KFK09\_013183, KFK09\_010477, as well as the PMK genes KFK09\_023365, KFK09\_015471, the IDI gene KFK09\_008671, and some of the TPS genes KFK09\_027207, KFK09\_023284, KFK09\_011873, and KFK09\_006206 (Figure 12). Although none of the relevant genes in the MVA pathway were enriched in the mediumpurple3 and darkorange modules, their significance should not be overlooked. This suggests that the variation in dendrobine content across different years cannot be attributed solely to any one pathway. Furthermore, the subsequent biological processes involved in the formation of dendrobine from the terpene skeleton remain unclear (Chen et al., 2021), indicating that genetic changes in the MVA pathway and MEP pathway do not constitute the sole correlation with dendrobine synthesis.

## 4 Discussion

Since ancestral plants settled on land 450 million years ago, they have been interacting with microorganisms to form a “holobiont” (Hassani et al., 2018). These ubiquitous interactions between microbial communities and their host plants often shape host

phenotypes and regulate metabolite synthesis (Sharma et al., 2021). Plants have evolved the ability to produce a large number of unique metabolites, and this metabolic diversification is likely driven by the need to adapt to different environments (Chae et al., 2014). One of the key environmental factors affecting plant health and adaptability is the host microbiota (Bulgarelli et al., 2012). Recent studies reveal an additional role for the plant-specialized metabolite camalexin in facilitating host-inter-root microbial interactions (Huang et al., 2019). However, how the microbial-host maintains homeostasis after perturbation remains poorly understood (Ma et al., 2021). Thus, the interaction between endophytic fungi and host has attracted wide attention, because they are a group of symbiotic fungi that colonize plant tissues and organs without causing apparent disease (Clay, 2004), but have the ability to reshape plant characteristics (Yan et al., 2019). There are two sides to every story. Endophytic fungi can provide various benefits to the host plant, such as promoting growth (Koberl et al., 2013; Shan et al., 2021), enhancing stress tolerance, inducing resistance (Ma et al., 2021) and producing bioactive compounds (Ancheeva et al., 2020). However, they also have negative effects on the host plant, conversion of endophytes from symbiotic to parasitic state (Thrall et al., 2007). Therefore, the interaction between endophytic fungi and host plant is complex and dynamic, and needs to be explored and understood in depth at different levels and scales.

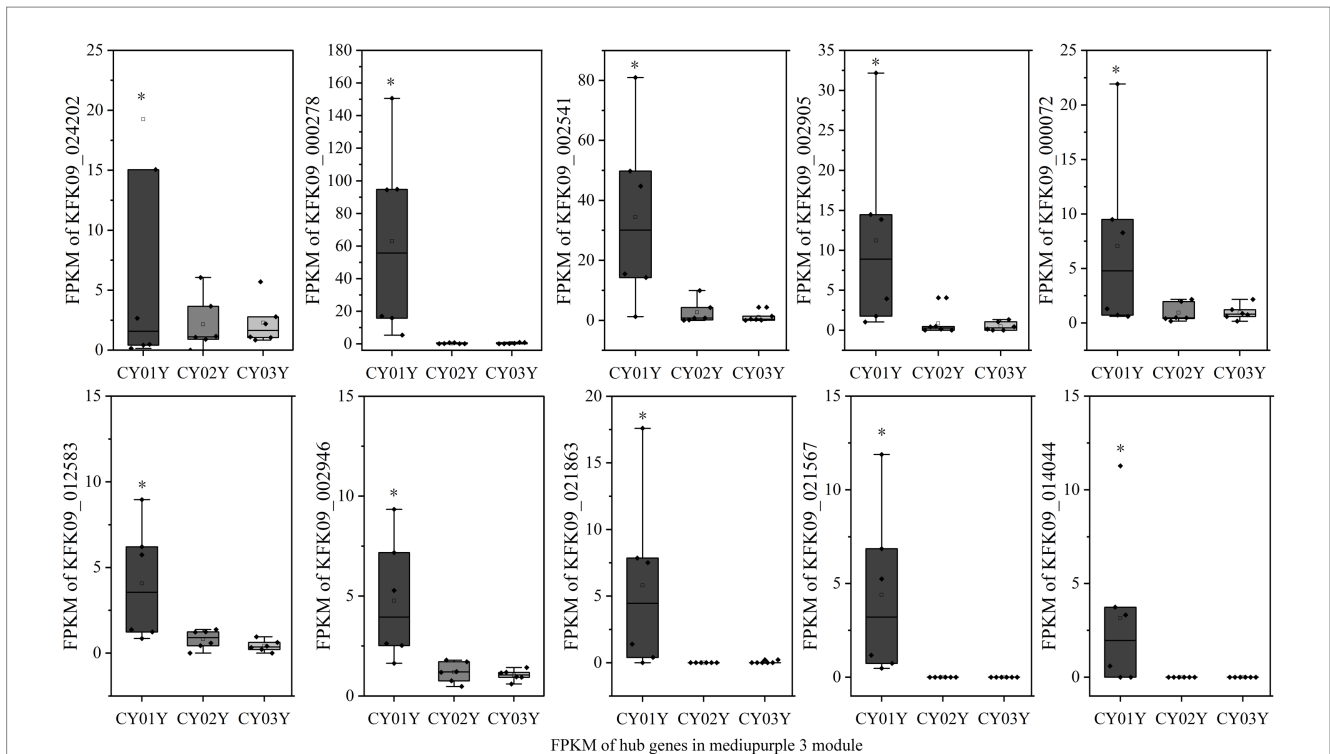


**FIGURE 10**  
The expression graph of 10 genes in the mediumpurple3 module. The diagram showed the gene expression is significantly higher in annuals than in 2- and 3-year olds (\* $p < 0.05$ ).

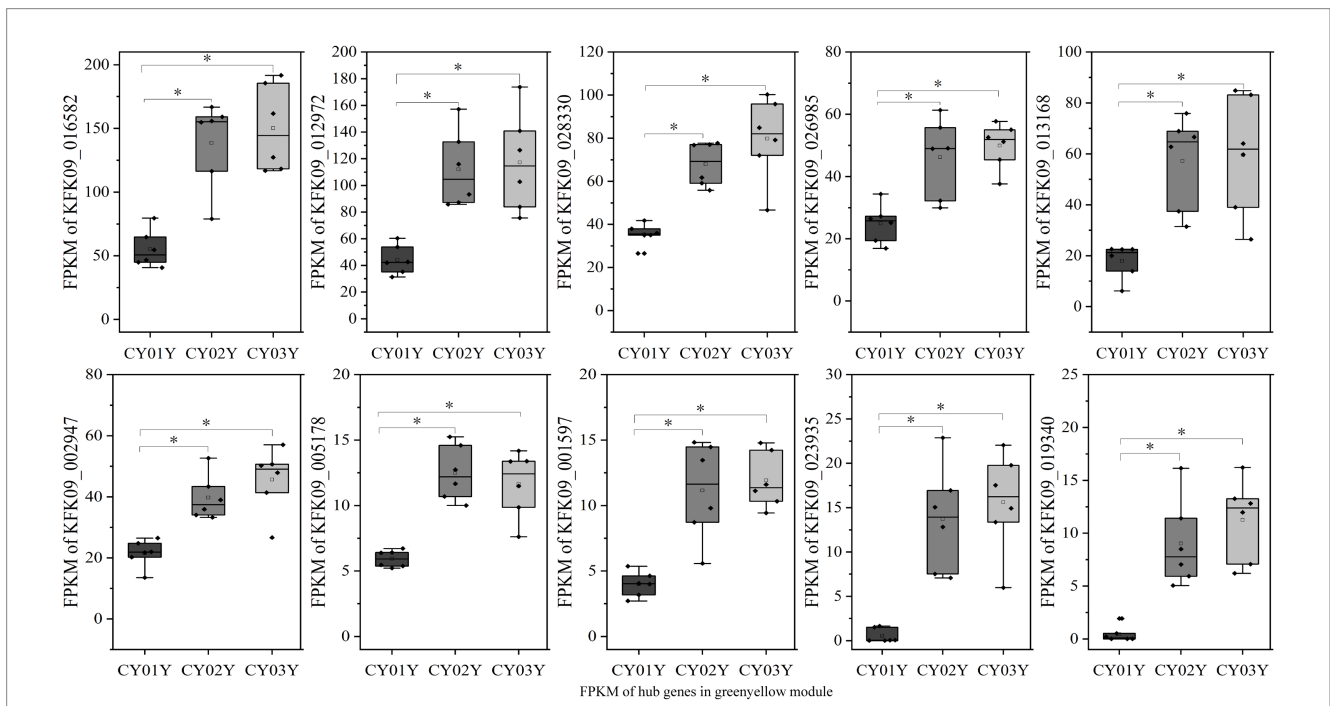


**FIGURE 11**  
The expression graph of 10 genes in the greenyellow module. The graph shows that the expression of genes increases with the age of the plant (\* $p < 0.05$ ).

*Dendrobium nobile* is a traditional Chinese medicinal herb with various pharmacological effects, mainly derived from its main active ingredient, dendrobine. However, the content of dendrobine in

*D. nobile* varies greatly with the age of the plant, and the underlying mechanism is still unclear (Gong et al., 2021). In this study, we observed significant shifts in the composition and abundance of

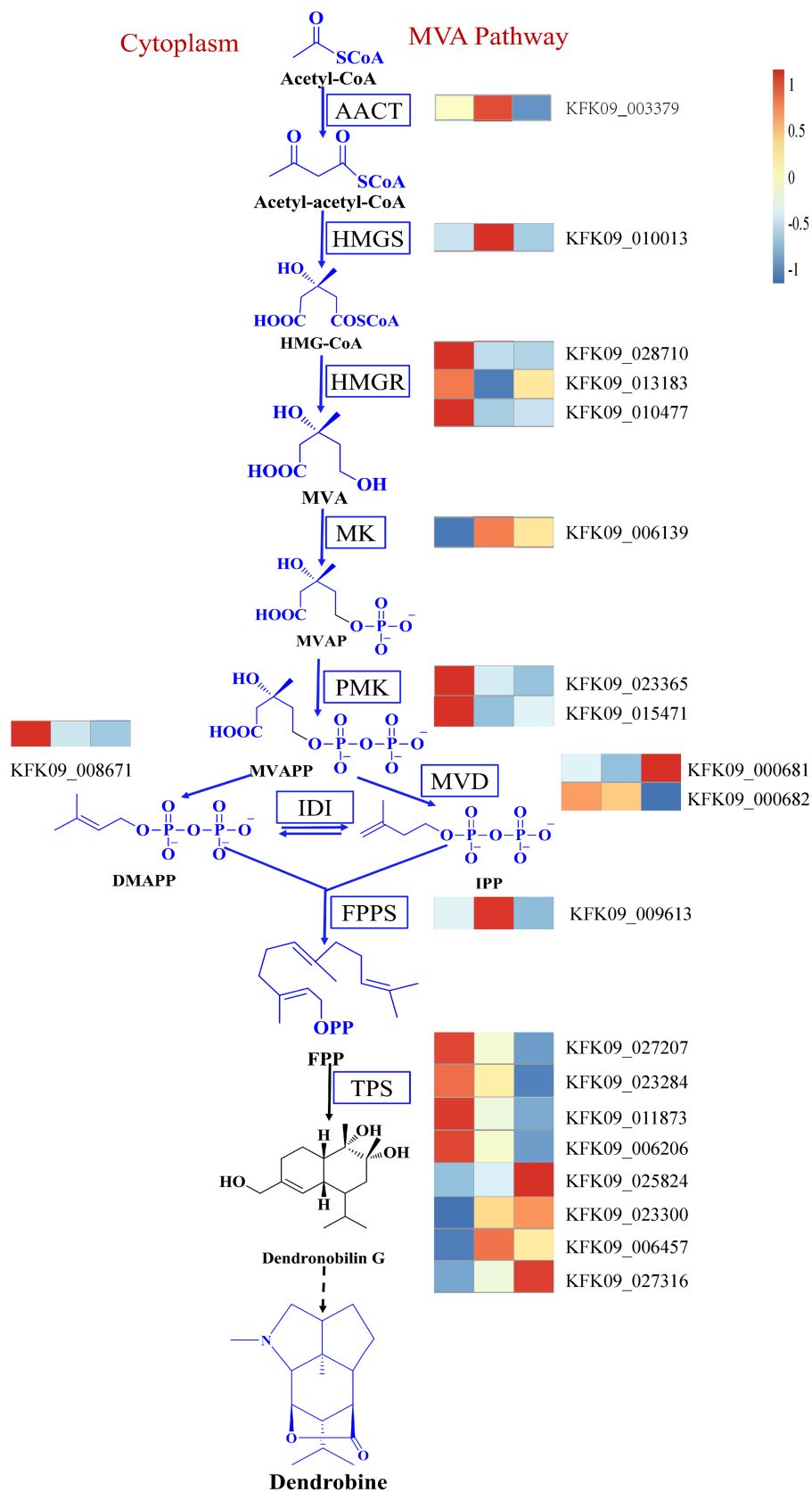


**FIGURE 12**  
 The MVA pathway of dendrobine and changes in key genes of the pathway. AACT, Acetoacetyl-CoA thiolase; HMGS, 3-hydroxy-3-methylglutaryl-coenzymeA synthase; HMGR, HMG-CoA reductase; MK, Mevalonate kinase. PMK, Phosphomevalonate kinase; MVD, Mevalonate diphosphate decarboxylase; IDI, Isopentenyl diphosphate isomerase; FPPS, Farnesyl diphosphate synthase; TPS, Terpenoid synthase.

endophytic fungi in the stems of *D. nobile* along the age axis, which correlated strongly with changes in the stem transcriptome. These findings are consistent with those of other studies on plants (Liu et al., 2017). Based on these observations, we hypothesized that age-dependent changes in the stem transcriptomes might be responsible for the observed variations in endophytic fungi. Several fungal genera, such as *Olpidium*, *Hannaella*, *Plectosphaerella*, *Strelitziana* and *Trichomerium*, were associated with different transcriptomic modules and dendrobine content. Meanwhile, some genes in plant hormone signaling and alkaloid biosynthesis pathways were differentially expressed among different ages and correlated with endophytic fungi and dendrobine content. Our results suggest that endophytic fungi may play an important role in regulating the stem transcriptome and dendrobine synthesis in *D. nobile* along the age gradient.

The co-occurrence network analysis revealed that the endophytic fungal community in the stems of *D. nobile* had a modularly structured according to different age groups. For instance, the 1-year-old *D. nobile* had a unique fungal community and corresponding transcriptomic module, which showed the highest correlation with *Olpidium*, *Hannaella*, and *Plectosphaerella* at the genus level compared to all other samples. *Olpidium* is known to act as a vector for plant viruses, infecting many plants with a wide range of hosts (Lay et al., 2018). At the level of species, there are *Olpidium brassicae* and *Olpidium virulentus* in the stems. *O. brassicae* and other *Olpidium* species sometimes form a large part of the fungal community in other plant roots or rhizospheres (Tkacz et al., 2015). *Hannaella*, which is a basidiomycetous yeast genus belonging to the order Tremellales, phylum Basidiomycota, had the highest abundance in *Alpinia zerumbet* (Yan et al., 2022) and *Salvia miltiorrhiza* (Chen et al., 2018). There are *Hannaella pagnoccae*, *Hannaella sinensis*, *Hannaella oryzae*, *Hannaella surugaensis*, *Hannaella luteola* and other species in our samples, and they all have been described in the *Hannaella* genus. Widespread on the leaf surfaces of various plants, including rice, wheat, and fruit trees (Han et al., 2017). *H. oryzae* was thought to play an important role in plant growth promotion and biocontrol as an important phyllosphere inhabiting yeast (Li Q. et al., 2021). The genus *Plectosphaerella* is the largest genus in the family Plectosphaerellaceae. Some species are plant pathogens, whereas others are soil-borne (Zhang et al., 2019). In the stem of *D. nobile*, several species were detected including *Plectosphaerella oratosquillae*, *Plectosphaerella oratosquillae* and *Plectosphaerella alismatis*. Most species of *Plectosphaerella* are pathogens causing large losses in agriculture reportedly (Yang et al., 2021). Therefore, according to the analysis, *Hannaella* is one of the endophytes instructive by subsequent studies. Moreover, module greenyellow had a significantly high correlation with fungus *Strelitziana*, *Trichomerium* in comparison with the 1-year ages. *Strelitziana* was found to be the dominant genus in plant biomass in muscadine grape skins (Sun et al., 2021) and *Pinus massoniana* (Chen et al., 2023), whereas *Trichomerium* was low in abundance in muscadine grape skins but played an important role in *Pinus massoniana*. Further investigation is needed to understand their effect on the host.

Recent evidence suggests that stress and defense response signaling play a role in the production of plant metabolites (SMs) (Isah, 2019). Fungal endophytes, as a phylogenetically and functionally diverse group, can interact with plants in various ways (Chen et al., 2022). Plants adjust their metabolism to environmental conditions, in

part through the recognition of a wide array of self and non-self molecules. Among them, endophytes are a provider of the non-self molecules (Bjornson et al., 2021). Differences in endophytic fungal species and abundance must necessarily induce a direct response to host transcription. The transcriptional landscape of *D. nobile* is significantly different along the ages axis with distinct endophytes, but the analysis of the transcriptional landscape is complicated due to the numerous influencing factors. An interesting syndrome came to light through the differential expression analysis of ASV as well as the module analysis of WGCNA. The following genes specificity was summarized in mediumpurple3 module and varied significantly among samples, and correlated with plant hormone metabolism. Plant hormones are a key signaling mechanism for plants to respond to external abiotic factors, and then regulate plant morphology, growth, and synthesis of secondary metabolites (Blazquez et al., 2020). They can also mediate the interaction between plants and microorganisms, either positively or negatively (Kou et al., 2021). In our study, we found that some genes involved in plant hormone signaling, such as NPR1, SAUR, AUX/IAA and ARE, were differentially expressed among different ages and correlated with endophytic fungi and dendrobine content. NPR1 (gene-KFK09\_020743) is a key node in signaling downstream from Salicylic acid (SA). It activates defense gene transcription under pathogen challenge (An and Mou, 2011). Auxin plays a crucial role in the process from embryogenesis to senescence in plants, much of which is achieved through the regulation of auxin response genes. As the largest family of early auxin response genes, gene KFK09\_019829 (small auxin upregulated RNA (SAUR)) plays an key role in plant growth and development (Li et al., 2021). Auxin-responsive protein IAA (AUX/IAA) Aux/IAA proteins are short-lived nuclear proteins comprising several highly conserved domains that are encoded by the auxin early response gene family (Luo et al., 2018). We designed primers for these four key genes for RT-PCR and obtained the same trend of changes as RNA-seq (Supplementary Figure S4). Further elaboration, they all are the key regulatory nodes of different plant hormones.

Alkaloids, a diverse group of nitrogen-containing secondary metabolites, exhibit a range of biological activities and pharmacological effects (Bhambhani et al., 2021). Among these alkaloids, dendrobine plays a crucial role in *Dendrobium nobile*, displaying antioxidant properties (Hsu et al., 2022) and hepatoprotective effects (Zhou et al., 2020). Despite its significance, the biosynthesis of dendrobine remains poorly understood, although it is hypothesized to involve two major pathways: the mevalonate (MVA) pathway and the methylerythritol phosphate (MEP) pathway (Gong et al., 2021). The MVA pathway generates isopentenyl diphosphate (IPP) and dimethylallyl diphosphate (DMAPP), which serve as precursors for terpenoids. On the other hand, the MEP pathway produces 1-deoxy-D-xylulose-5-phosphate (DXP), a precursor for plastidial terpenoids. Both pathways converge at geranyl diphosphate (GPP), which is subsequently converted to dendrobine by terpene synthases (TPS) and other enzymes. In our study, we observed differential expression of genes involved in alkaloid biosynthesis pathways, such as HMGR, PMK, IDI and TPS, were differentially expressed among different ages and correlated with endophytic fungi and dendrobine content. HMGR, a key enzyme in the MVA pathway, catalyzes the conversion of 3-hydroxy-3-methylglutaryl-CoA (HMG-CoA) to mevalonate (MVA). PMK, an enzyme in the MVA pathway, catalyzes the phosphorylation of mevalonate to mevalonate-5-phosphate (MVP). IDI is an enzyme that

catalyzes the interconversion of IPP and DMAPP. TPS is a family of enzymes that catalyze the formation of various terpenoids from GPP or other prenyl diphosphates. The differential expression of these genes suggests that *D. nobile* exhibits varying capacities for alkaloid biosynthesis at different ages, influenced by the composition and abundance of the endophytic fungal community.

## 5 Conclusion

Our study provides novel insights into the interaction between endophytic fungi and the host plant, *D. nobile*, along the age gradient. Our results suggest that endophytic fungi may influence the transcriptome of the stem and the synthesis of dendrobine in *D. nobile* by modulating plant hormone signaling and alkaloid biosynthesis pathways. Additionally, we have identified specific fungal genera and gene modules that are associated with dendrobine content. These findings have potential implications for enhancing the quality and yield of *D. nobile* through targeted manipulation of the endophytic fungal community or host plant gene expression. However, it is important to acknowledge the limitations and uncertainties of our study, which should be addressed in future research. Firstly, our sampling was limited to the stems of *D. nobile* at three different ages, which may not fully represent the entire life cycle of the plant, although these ages are typically harvested within 3 years. It would be valuable to expand the sampling to include a broader range of ages and other tissues, such as roots and flowers, to obtain a more comprehensive understanding of the dynamics of the endophytic fungal community and transcriptome in *D. nobile*. Secondly, we solely employed ITS sequencing to identify the endophytic fungi in the stems of *D. nobile*, which may not capture the complete diversity and functionality of the fungal community. It would be beneficial to incorporate other molecular markers or metagenomic approaches to unveil the functional genes and metabolic pathways of the endophytic fungi in *D. nobile*.

## Data availability statement

The data presented in the study are deposited in the NCBI repository, BioProject ID: PRJNA1040334, SRA: SRR26830466, <https://submit.ncbi.nlm.nih.gov/subs/bioproject/SUB13972852/overview>.

## Author contributions

YZ: Data curation, Writing – original draft. XJ: Validation, Writing – original draft. XL: Validation, Writing – original draft. LQ: Data curation, Writing – review & editing. DT: Methodology, Writing – review & editing. DW: Validation, Writing – review & editing. CB:

## References

- Afkhami, M. E., and Strauss, S. Y. (2016). Native fungal endophytes suppress an exotic dominant and increase plant diversity over small and large spatial scales. *Ecology (Durham)* 97, 1159–1169. doi: 10.1890/15-1166.1
- An, C., and Mou, Z. (2011). Salicylic acid and its function in plant immunity. *J. Integr. Plant Biol.* 53, 412–428. doi: 10.1111/j.1744-7909.2011.01043.x
- Ancheeva, E., Daletos, G., and Proksch, P. (2020). Bioactive secondary metabolites from endophytic fungi. *Curr. Med. Chem.* 27, 1836–1854. doi: 10.2174/0929867326666190916144709
- Bhambhani, S., Kondhare, K. R., and Giri, A. P. (2021). Diversity in chemical structures and biological properties of plant alkaloids. *Molecules* 26:374. doi: 10.3390/molecules26113374

Resources, Writing – review & editing. JY: Resources, Writing – review & editing. JX: Supervision, Writing – review & editing. YH: Conceptualization, Funding acquisition, Visualization, Writing – review & editing.

## Funding

The author(s) declare financial support was received for the research, authorship, and/or publication of this article. This research was funded by the National Nature Science Foundation of China (82160812), Guizhou Engineering Research Center of Industrial Key-technology for *Dendrobium nobile* [QJJ(2022)048, QJJ(2022)006], the Department of Science and Technology of Guizhou Province [QKHZC (2021)420, QKHZC (2023)261].

## Acknowledgments

We would like to thank Guangxi Shenli Pharmaceutical Co., Ltd. and Chishui Xintian Chinese Medicine Industry Development Co., Ltd. for providing *Dendrobium nobile*.

## Conflict of interest

CB was employed by Guangxi Shenli Pharmaceutical Co., Ltd. JY was employed by Chishui Xintian Chinese Medicine Industry Development Co., Ltd.

The remaining authors declare that the research was conducted in the absence of any commercial or financial relationships that could be construed as a potential conflict of interest.

## Publisher's note

All claims expressed in this article are solely those of the authors and do not necessarily represent those of their affiliated organizations, or those of the publisher, the editors and the reviewers. Any product that may be evaluated in this article, or claim that may be made by its manufacturer, is not guaranteed or endorsed by the publisher.

## Supplementary material

The Supplementary material for this article can be found online at: <https://www.frontiersin.org/articles/10.3389/fmicb.2023.1294402/full#supplementary-material>

- Bjornson, M., Pimprikar, P., Nürnberger, T., and Zipfel, C. (2021). The transcriptional landscape of *Arabidopsis thaliana* pattern-triggered immunity. *Nature Plants* 7, 579–586. doi: 10.1038/s41477-021-00874-5
- Blazquez, M. A., Nelson, D. C., and Weijers, D. (2020). Evolution of plant hormone response pathways. *Annu. Rev. Plant Biol.* 71, 327–353. doi: 10.1146/annurev-arplant-050718-100309
- Bulgarelli, D., Rott, M., Schlaeppi, K., Van Themaat, V. L., Ahmadinejad, N., Assenza, F., et al. (2012). Revealing structure and assembly cues for *Arabidopsis* root-inhabiting bacterial microbiota. *Nature* 488, 91–95. doi: 10.1038/nature11336
- Chae, L., Kim, T., Nilo-Poyanco, R., and Rhee, S. Y. (2014). Genomic signatures of specialized metabolism in plants. *Science* 344, 510–513. doi: 10.1126/science.1252076
- Chen, X., Li, Q., Xu, X., Ding, G., Guo, S., and Li, B. (2021). Effects of the endophytic fungus mf23 on *Dendrobium nobile* Lindl. in an artificial primary environment. *ACS Omega* 6, 10047–10053. doi: 10.1021/acsomega.0c06325
- Chen, K. H., Liao, H. L., Arnold, A. E., Korotkin, H. B., Wu, S. H., Matheny, P. B., et al. (2022). Comparative transcriptomics of fungal endophytes in co-culture with their moss host *Dicranum scoparium* reveals fungal trophic lability and moss unchanged to slightly increased growth rates. *New Phytol.* 234, 1832–1847. doi: 10.1111/nph.18078
- Chen, H., Wu, H., Yan, B., Zhao, H., Liu, F., Zhang, H., et al. (2018). Core microbiome of medicinal plant *Salvia miltiorrhiza* seed: a rich reservoir of beneficial microbes for secondary metabolism? *Int. J. Mol. Sci.* 19:672. doi: 10.3390/ijms19030672
- Chen, H., Zhang, L., Huang, Z., Wu, Z., Tan, M., Zhang, X., et al. (2023). Effect of anoxic atmosphere on the physicochemical and pelletization properties of *Pinus massoniana* sawdust during storage. *Int. J. Environ. Res. Public Health* 20:791. doi: 10.3390/ijerph20010791
- Clay, K. (2004). Fungi and the food of the gods. *Nature* 427, 401–402. doi: 10.1038/427401a
- Clay, K., and Holah, J. (1999). Fungal endophyte symbiosis and plant diversity in successional fields. *Science* 285, 1742–1744. doi: 10.1126/science.285.5434.1742
- Gong, D. Y., Chen, X. Y., Guo, S. X., Wang, B. C., and Li, B. (2021). Recent advances and new insights in biosynthesis of dendrobine and sesquiterpenes. *Appl. Microbiol. Biotechnol.* 105, 6597–6606. doi: 10.1007/s00253-021-11534-1
- Han, L., Li, Z., Guo, X., Tan, J., He, S., Cui, X. L., et al. (2017). *Hannaella dianchiensis* sp. nov., a basidiomycetous yeast species isolated from lake water. *Int. J. Syst. Evol. Microbiol.* 67, 2014–2018. doi: 10.1099/ijsem.0.001908
- Harrison, J. G., Beltran, L. P., Buerkle, C. A., Cook, D., Gardner, D. R., Parchman, T. L., et al. (2021). A suite of rare microbes interacts with a dominant, heritable, fungal endophyte to influence plant trait expression. *ISME J.* 15, 2763–2778. doi: 10.1038/s41396-021-00964-4
- Hassani, M. A., Durán, P., and Hacquard, S. (2018). Microbial interactions within the plant holobiont. *Microbiome* 6:58. doi: 10.1186/s40168-018-0445-0
- Hsu, W. H., Chung, C. P., Wang, Y. Y., Kuo, Y. H., Yeh, C. H., Lee, I. J., et al. (2022). *Dendrobium nobile* protects retinal cells from UV-induced oxidative stress damage via nrf2/ho-1 and mapk pathways. *J. Ethnopharmacol.* 288:114886. doi: 10.1016/j.jep.2021.114886
- Huang, A. C., Jiang, T., Liu, Y., Bai, Y., Reed, J., Qu, B., et al. (2019). A specialized metabolic network selectively modulates *Arabidopsis* root microbiota. *Science* 364:6389. doi: 10.1126/science.aau6389
- Isah, T. (2019). Stress and defense responses in plant secondary metabolites production. *Biol. Res.* 52:39. doi: 10.1186/s40659-019-0246-3
- Koberl, M., Schmidt, R., Ramadan, E. M., Bauer, R., and Berg, G. (2013). The microbiome of medicinal plants: diversity and importance for plant growth, quality and health. *Front. Microbiol.* 4:400. doi: 10.3389/fmicb.2013.00400
- Kou, M., Bastias, D. A., Christensen, M. J., Zhong, R., Nan, Z., and Zhang, X. X. (2021). The plant salicylic acid signalling pathway regulates the infection of a biotrophic pathogen in grasses associated with an epichloë endophyte. *J. Fungi* 7:633. doi: 10.3390/jof7080633
- Lay, C., Hamel, C., and St-Arnaud, M. (2018). Taxonomy and pathogenicity of ophioidium brassicae and its allied species. *Fungal Biol.* 122, 837–846. doi: 10.1016/j.funbio.2018.04.012
- Li, M., Chen, R., Gu, H., Cheng, D., Guo, X., Shi, C., et al. (2021). Grape small auxin upregulated rna (saur) 041 is a candidate regulator of berry size in grape. *Int. J. Mol. Sci.* 22:11818. doi: 10.3390/ijms222111818
- Li, Q., Li, L., Feng, H., Tu, W., Bao, Z., Xiong, C., et al. (2021). Characterization of the complete mitochondrial genome of basidiomycete yeast *Hannaella oryzae*: intron evolution, gene rearrangement, and its phylogeny. *Front. Microbiol.* 12:567. doi: 10.3389/fmicb.2021.646567
- Liu, T., Greenslade, A., and Yang, S. (2017). Levels of rhizome endophytic fungi fluctuate in *Paris polyphylla* var. *Yunnanensis* as plants age. *Plant Divers.* 39, 60–64. doi: 10.1016/j.pld.2016.11.006
- Lu, A. J., Jiang, Y., Wu, J., Tan, D. P., Qin, L., Lu, Y. L., et al. (2022). Opposite trends of glycosides and alkaloids in *Dendrobium nobile* of different age based on uplc-q/tof-ms combined with multivariate statistical analyses. *Phytochem. Anal.* 33, 619–634. doi: 10.1002/pca.3115
- Luo, J., Zhou, J., and Zhang, J. (2018). Aux/iaa gene family in plants: molecular structure, regulation, and function. *Int. J. Mol. Sci.* 19:259. doi: 10.3390/ijms19010259
- Ma, K., Niu, Y., Jia, Y., Ordon, J., Copeland, C., Emonet, A., et al. (2021). Coordination of microbe–host homeostasis by crosstalk with plant innate immunity. *Nat. Plants* 7, 814–825. doi: 10.1038/s41477-021-00920-2
- Shan, T., Zhou, L., Li, B., Chen, X., Guo, S., Wang, A., et al. (2021). The plant growth-promoting fungus mf23 (*Mycena* sp.) increases production of *Dendrobium officinale* (orchidaceae) by affecting nitrogen uptake and nh<sub>4</sub><sup>+</sup> assimilation. *Front. Plant Sci.* 12:693561. doi: 10.3389/fpls.2021.693561
- Sharma, H., Rai, A. K., Dahiya, D., Chettri, R., and Nigam, P. S. (2021). Exploring endophytes for in vitro synthesis of bioactive compounds similar to metabolites produced in vivo by host plants. *Aims Microbiol.* 7, 175–199. doi: 10.3934/microbiol.2021012
- Sun, D., Qu, J., Huang, Y., Lu, J., and Yin, L. (2021). Analysis of microbial community diversity of muscadine grape skins. *Food Res. Int.* 145:110417. doi: 10.1016/j.foodres.2021.110417
- Teixeira, D. S. J., and Ng, T. B. (2017). The medicinal and pharmaceutical importance of *Dendrobium* species. *Appl. Microbiol. Biotechnol.* 101, 2227–2239. doi: 10.1007/s00253-017-8169-9
- Thrall, P. H., Hochberg, M. E., Burdon, J. J., and Bever, J. D. (2007). Coevolution of symbiotic mutualists and parasites in a community context. *Trends Ecol. Evol.* 22, 120–126. doi: 10.1016/j.tree.2006.11.007
- Tkacz, A., Cheema, J., Chandra, G., Grant, A., and Poole, P. S. (2015). Stability and succession of the rhizosphere microbiota depends upon plant type and soil composition. *ISME J.* 9, 2349–2359. doi: 10.1038/ismej.2015.41
- Wang, Z., Zhao, M., Cui, H., Li, J., and Wang, M. (2020). Transcriptomic landscape of medicinal *Dendrobium* reveals genes associated with the biosynthesis of bioactive components. *Front. Plant Sci.* 11:391. doi: 10.3389/fpls.2020.00391
- Yan, K., Pei, Z., Meng, L., Zheng, Y., Wang, L., Feng, R., et al. (2022). Determination of community structure and diversity of seed-vectored endophytic fungi in *Alpinia zerumbet*. *Front. Microbiol.* 13:864. doi: 10.3389/fmicb.2022.814864
- Yan, L., Zhu, J., Zhao, X., Shi, J., Jiang, C., and Shao, D. (2019). Beneficial effects of endophytic fungi colonization on plants. *Appl. Microbiol. Biotechnol.* 2019:713. doi: 10.1007/s00253-019-09713-2
- Yang, X. Q., Ma, S. Y., Peng, Z. X., Wang, Z. Q., Qiao, M., and Yu, Z. (2021). Diversity of *Plectosphaerella* within aquatic plants from Southwest China, with *P. Endophytica* and *P. Sichuanensis* spp. *Myckeys* 80, 57–75. doi: 10.3897/mycokeys.80.64624
- Zhang, Z., Chen, W., Zou, X., Han, Y., Huang, J., Liang, X. Q., et al. (2019). Phylogeny and taxonomy of two new *Plectosphaerella* (Plectosphaerellaceae, Glomerellales) species from China. *Myckeys* 57, 47–60. doi: 10.3897/mycokeys.57.36628
- Zhao, Y., Qin, L., Tan, D., Wu, D., Wu, X., Fan, Q., et al. (2023). Fatty acid metabolites of *Dendrobium nobile* were positively correlated with representative endophytic fungi at altitude. *Front. Microbiol.* 14:956. doi: 10.3389/fmicb.2023.1128956
- Zhou, J., Zhang, Y., Li, S., Zhou, Q., Lu, Y., Shi, J., et al. (2020). *Dendrobium nobile* Lindl. Alkaloids-mediated protection against ccl4-induced liver mitochondrial oxidative damage is dependent on the activation of nrf2 signaling pathway. *Biomed. Pharmacother.* 129:110351. doi: 10.1016/j.biopha.2020.110351